Advances in Modelling and Analysis B
Vol. 61, No. 3, September, 2018, pp. 113-118
Journal homepage:http://iieta.org/Journals/AMA/AMA_B

Fusion of multispectral and panchromatic images based on entropy and fruit fly optimization

Abdelwhab Ouahab*, Mohamed F. Belbachir

Laboratoire Signaux, Systèmes et Données (LSSD), Université des Sciences et de la Technologie d'Oran Mohamed Boudiaf, USTO-MB, BP 1505, El M'naouer, Oran 31000, Algérie

Corresponding Author Email: ouahab.abdelwhab@univ-usto.dz

https://doi.org/10.18280/ama_b.610301

Received: 11 July 2018
Accepted: 5 September 2018

Keywords:
image fusion, pansharpening, entropy, fruit fly optimization

ABSTRACT

Image fusion (pan-sharpening) aims to generate a single image from both a panchromatic (PAN) image and multispectral images (MS). The pan-sharpened images ought to be identical to the MS images in terms of spectral information and ought also to be similar to the PAN image in terms of spatial information. Different fusion methods and algorithms have been purposed in the literature such as intensity-hue-saturation (IHS), wavelet transform (WT), principal component analysis (PCA) and Brovey transform (BT), etc. These techniques can produce color distortions in the fused images. This problem is principally due to the fact that the same details extracted from the PAN image are injected into each band of the MS images. FUFSER method utilizes the spectral response functions and Fourier transform (FT) to make an injection model. A new fusion method based on FUFSER method is presented in order to improve the spatial and spectral qualities of the fused images. This method usees local and global parameters to compute the amount of spatial details extracted from the PAN image to be added into each band of the MS images. The global parameters are computed using the fruit fly optimization, whereas the local parameters are computed using the entropy. The proposed method is applied to Pléiades and IKONOS images and compared with some existing fusion methods. The results obtained showed that the proposed method has better performance compared than other methods in terms of spatial and spectral information.

1. INTRODUCTION

There are various remote sensing satellites that provide multispectral images (MS) with a lower spatial resolution and panchromatic images (PAN) with a higher spatial resolution such as the IKONOS, Pléiades, QuickBird, and GEOYE-1 [1]. Pansharpening allows to generate multispectral images with high-resolution information [2]. It is utilized in different applications such as surveillance and mapping. Various methods and strategies have been proposed in the literature to do this operation [3].

The Brovey transform (BT) [4], Intensity-hue-saturation (IHS) [5], and Principal Component Analysis (PCA) [6] are among the oldest fusion methods. The disadvantages of these methods are that the fused images generated have more spectral distortions. The wavelet transform (WT) [1] and Fourier transform (FT) [7] preserve more of the spectral characteristics of the multispectral images. The Window Spectral Response (WiSpeR) fusion method uses the physical spectral response of sensors to compute the portion of spatial details extracted from the PAN image to be transferred into each band of the MS images [8]. However, this method incorporates the same details in each band of the MS images that can produce a spatial artifact. The FUFSER method is a combination of two methods (WiSpeR and Fourier transform) [9]. The injection coefficients in the WiSpeR and FUFSER methods are given globally, but the local analysis can generally perform better than the global analysis, Because the local analysis can reduce the divergence of the estimate and take local characteristics of images [10].

In order to benefit from the local analysis, we develop a modified version of the FUFSER method, in which we utilize two parameters to calculate the amount of spatial details extracted from the PAN image to be added into each band of the MS images. We utilize global and local parameters instead of using only global ones as in FUFSER methods. The global parameters are computed using the fruit fly optimization (FFO), whereas the local parameters are computed using the local entropy. The proposed approach is applied on IKONOS and Pléiades images and compared with some existing fusion methods.

2. FRUIT FLY OPTIMIZATION (FFO)

The FFO method is among of the latest developed methods which is created by WenchaoPan [12-11] for resolving global optimization problems. It is based on the foraging behavior of the fruit fly. This method has numerous advantages such as fast convergence, a simple computational operation, and fewer influential parameters. Fruit fly can displace a short distance to look for food locations [13]. According to this principle, the basic steps of FFO are:

(1) Initialize parameters: The size of the population (sizepop), the maximal iteration number of FFO (MaxGen), and the fruit fly group's location x_{axis}, y_{axis}.

(2) Each fruit fly displaces randomly to look for the food by using osphresis. A new position is calculated using Eq. (1).

$$x_i = x_{axis} + RandomValue$$
$$y_i = y_{axis} + RandomValue \quad (1)$$

(3) Calculate the distance of the food to the origin ($Dist_i$). After that, the value of the smell concentration Si is calculated by Eq. (2).

$$Dist_i = \sqrt{(x_i^2 + y_i^2)}$$
$$S_i = 1/Dist_i \quad (2)$$

(4) Substitue smell concentration value (S_i) into smell concentration function to generate the smell concentration of each fruit fly (Smelli):

$$Smell_i = fonction(S_i) \quad (3)$$

(5) Choose the fruit fly which has the smallest smell concentration:

$$[bestSmell, bestIndex] = \min(Smell_i) \quad (4)$$

(6) Save the best smell concentration and its location, then the fruit fly displaces towards that location by using vision.

$$x_{axis} = x(bestIndex)$$
$$y_{axis} = y(bestIndex) \quad (5)$$

(7) Alterate step two to step six until the fixed iteration number is arrived

3. THE PROPOSED FUSION METHOD

The general fusion framework is that the fused image can be decomposed into high and low-frequency information [14].

$$F_n = high(F_n) + low(F_n) \quad (6)$$

where $high(F_n)$ is the high frequency information of the nth band of the fused image and $low(F_n)$ is the low frequency information of the nth band of the fused image. The high and low frequency information can be extracted from the PAN and the MS images. For that, Eq. (6) can be written as in [15], as follows:

$$F_n = high(F_n) + low(F_n) \quad (7)$$

$$\approx \delta_n high(PAN) + low(MS_n^z) \quad (8)$$

where MS^z are the upsampled MS images, δ_n is reflects the amount of spatial details extracted from the PAN image to be incorporated into nth band of the MS images. We show that $\delta_n$is a global parameter injection, which is related to the entire band. The parameter δ_n cannot produce good quality of the fused image because it does not take the local characteristics of the MS images, especially when the MS images contains more textured regions. To use the local characteristics of the MS images, we introduce new fusion parameters $\partial_n(i,j)$ that are calculated in a small window. For this Eq. (8) can be rewritten as:

$$F_n(i,j) \approx \delta_n \, \partial_n(i,j) high(PAN) + low(MS_n^z) \quad (9)$$

where $\partial_n(i,j)$ is a local fusion parameter of the nth band at location (i, j). We explain bellow how to compute each term in Eq. (9) and the flowchart of the proposed fusion method, which illustrates Eq. (9) is shown in Figure 1.

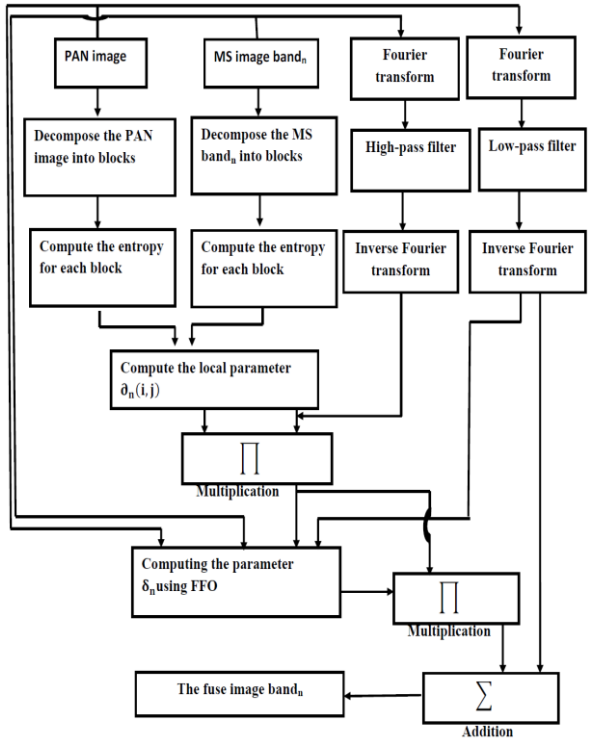

Figure 1. Flowchart of the proposed fusion method

3.1 The global parameter computation δ_n using the FFO

δ_n is generally calculated using an optimization method, or statistical method [15]. Here, we utilize the FFO to compute δ_n [16], because the SRF of the sensors in FUFSER method may not be appropriately evaluated for each image. δ_n takes values between zeros and one. We select the value of δ_n that maximize the following objective function:

$$O = SCC + CC \quad (10)$$

where SCC (the spatial correlation coefficient) and CC (the correlation coefficient) are explained in section 4.3.

Note that, the objective function O is a linear combination of two metrics. The first metric is utilized to estimate the spatial qualities of the merged images. The second parameter is utilized to estimate the spectral qualities of the merged images. The optimization of O can provide fused images with good spectral and spatial qualities.

3.2 The local fusion parameter compotation $\partial_n(i,j)$ by entropy

Entropy has been proposed for the first time by Claude Shannon in the quantification of information. Entropy evaluates the average of the information content of an image.The fused image should be containing more information [17]. The entropy of an image is defined as following:

$$entropy\ (image) = -\sum_{q=0}^{N-1} P_q \log(P_q) \quad (11)$$

where N is the total number of grey levels in the image and P_q the probability of grey level q in the image. We use below the entropy for estimating the local parameters for injecting detail to each band of the MS images.

In this section, we propose a new way to compute the local fusion parameter $\partial_n(i,j)$ .This parameter is computed on the basis of the amount of information contained in each band of the MS and the PAN images.

The objective of using entropy is to take the local characteristics of an image, which can enhance the qualities of the fused images [15].

Let the events em_n and ep that represent the amount of information contained in the MS_n^z and PAN images respectively.

The probability of an event em_n is:

$$p(em_n) = entropy(MS_n^z) \quad (12)$$

The probability of event ep is:

$$p(ep) = entropy(PAN) \quad (13)$$

The conditional probability of ep given em_n is defined to be:

$$p(ep/em_n) = \frac{p(em_n \cap ep)}{p(em_n)} \quad (14)$$

where

$$p(em_n \cap ep) = \min(entropy(ep), entropy(em_n)) \quad (15)$$

$p(ep/em_n)$ represents a single value for each MS image band. In order to compute $p(ep/em_n)$ locally, we decompose both MS_n^z and PAN images into blocks with size B x B and we calculate $p(ep/em_n)$ for each block. Therefore, Eq. (14) can be rewritten as follows:

$$p(ep_k/em_{n,k}) = \frac{p(em_{n,k} \cap ep_k)}{p(em_{n,k})} \quad (16)$$

where $p(em_{n,k} \cap ep_k)$=min(entropy(ep_k), entropy($em_{n,k}$)) and k is the k-th block.

Equation (16) means that if the entropy value of the k-th block in the MS_n image is greater than the entropy value of its corresponding block in the PAN image. The local parameter values for all pixels contained in this block are equal to one. In this case, the amount of spatial details from the PAN image to be transferred into the MS images are related only to the global parameters.

So, the local fusion parameter at location (i,j) is estimated as:

$$\partial_n(i,j) = p(ep_k/em_{n,k}) \quad (17)$$

Equation (17) means that the local parameters of all pixels contained in the k-th block are the same.

3.3 Low pass filter $low(MS_n^z)$

The MS images contain some high-frequency information. We applied a low pass filter to eliminate this high-frequency information.

The MS images are transformed into Fourier domain, after that the low-frequency filter is performed. Finally, the inverse FT is applied [9].

3.4 High-frequency extraction high(PAN)

In order to maintain the spectral proprieties of the MS images, only high-frequency information extracted from PAN image are added to the MS images [9].

The PAN image is transformed into Fourier domain, after that the high pass filter is performed. Finally, the inverse Fourier transform is performed.

4. EXPERIMENT RESULTS

The experiments were carried out on IKONOS and Pléiades datasets. These datasets were provided by European space agency (ESA). Each MS image band was upsampled to the pixel size of the PAN image using bicubic interpolation. The used images are shown in Figure 2.

The parameters selection

The experiment parameters are set as follows: The maximal iteration number (MaxGen) is set to 20), the size of the population (sizepop) is set to 10, the fruit fly group's location x_{axis}, y_{axis} take random values between 0 and 1.

A similar work in [15] that uses a local analysis for image fusion deduced that the block size between 9 and 11 gives the best result for image fusion. For that, we used this block size in our work to compute the local entropy.

In order to assess the robustness and effectiveness of the proposed method, we compared it with some existing fusion methods, i.e. PCA [18-19] the generalized IHS (GIHS) [16], the generalized IHS using spectral response functions (GIHS-SRF) [16], Wavelet Transform (WT) [6], Brovey [4-20], Gram Schmidt Adaptive (GSA) [19-21] and FUFSER [9].

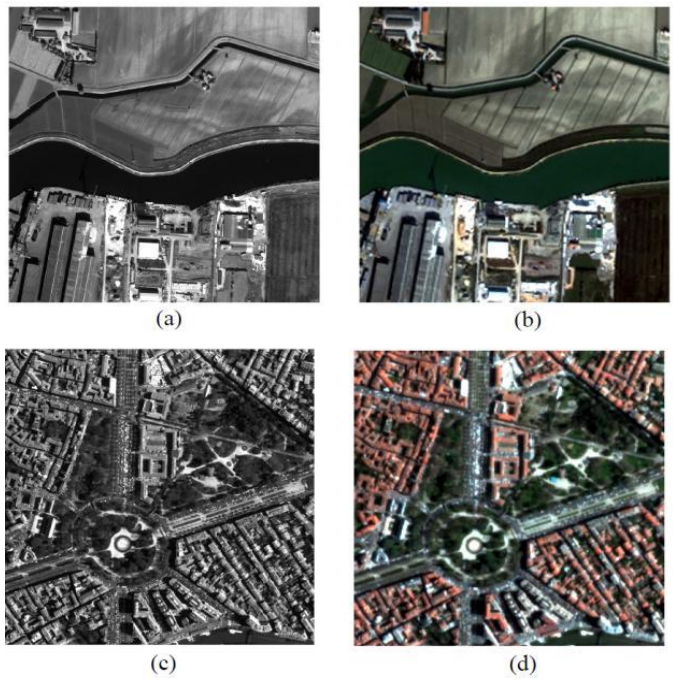

Figure 2. (a) IKONOS PAN image, (b) IKONOS MS images, (c) Pléiades PAN image, (d) Pléiades MS images

4.1 Visual analysis

Visual analysis of the fused images obtained by using different datasets on a selected region are shown in Figures 3 and 4.

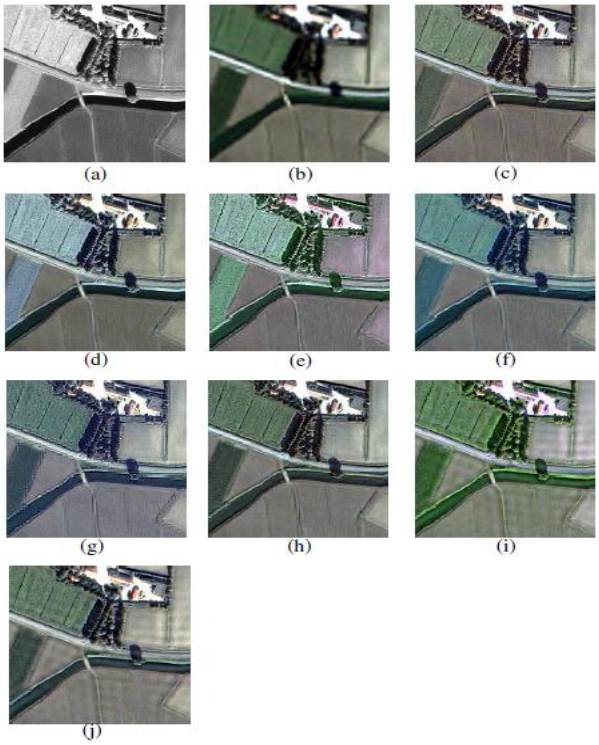

Figure 3. Selected region of the fused IKONOS images :(a) PAN image, (b) MS images, (c) PCA, (d) GIHS-SRF, (e) GIHS, (f) WT, (g) Brovey, (h) GSA, (i) FUFSER, (j) Proposed method

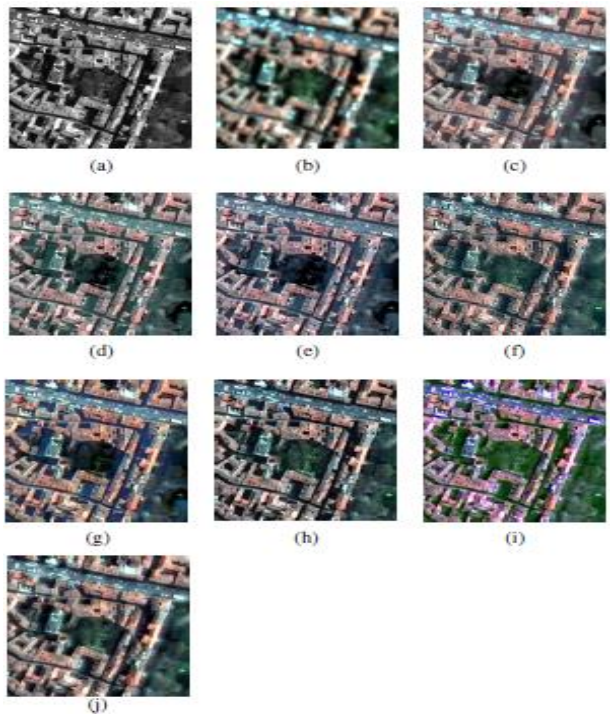

Figure 4. Selected region of the fused Pléiades images: (a) PAN image, (b) MS images, (c) PCA, (d) GIHS-SRF, (e) GIHS, (f) WT, (g) Brovey, (h) GSA, (i) FUFSER, (j) Proposed method

It can be seen that the spatial details extracted from the PAN image were introduced in the results obtained using all fusion methods. Obviously, the GIHS-SRF, GIHS and Brovey produce color distortion, that is especially clear in the vegetated area. WT produce fused images with less spatial details. FUFSER method has an excessive luminance. GSA preserve the color information well. PCA produces a blur on the fused images, that is clear in the results obtained on the Pléiades datasets as shown in Figure 4(c). The proposed method produces images with very good spatial details and less spectral distortions, as shown in Figures 3(j) and 4(j).

4.2 Quantitative evaluation

Five metrics are used to measure the performance of the proposed method.

4.2.1 Correlation coefficient metric (CC) [22-23]

The CC between the MS images and the fused image (F) is computed as follows:

$$CC(MS_i, F_i) = \frac{\sum_{k=1}^{N}\sum_{i=1}^{M}(MS_i(k,j)-\mu(MS_i))(F_i(k,j)-\mu(F_i))}{\sqrt{\sum_{j=1}^{N}\sum_{k=1}^{M}(MS_i(k,j)-\mu(MS_i))^2 \sum_{j=1}^{n}\sum_{i=1}^{m}(F_i(k,j)-\mu(F_i))}} \quad (18)$$

where $\mu(MS_i)$, $\mu(F_i)$ are the averages of MS_i and F_i respectively.

The CC takes a value in the range 1 and -1. The value of CC is near or equal to 1 indicate that the fused is good spectrally.

4.2.2 Spatial correlation coefficient metric (CC) [24]

The fused and panchromatic images are filtered by using Laplacian filter. Afterward, the CC is computed by the result of the filtered images. The value of SCC is near or equal to one for good spatial quality of the merged image.

4.2.3 Root mean square error metric (RMSE)

It is a popular metric for image evaluation. It's used to estimate the degree of color distortion in the merged image. Its formula is given as follows:

$$RMSE(MS_i, F_i) = \sqrt{\frac{\sum_{j=1}^{N}\sum_{k=1}^{M}(F_i(j,k)-MS_i(j,k))^2}{N\times M}} \quad (19)$$

where $N \times M$ are the number of pixels in the fused image.

4.2.4 Relative global synthesis error metric (ERGAS) [25]

It is used to estimate the spectral quality of the fused images. Its formula is given as follows:

$$ERGAS = 100\frac{p}{l}\sqrt{\frac{1}{N\times M}\sum_{i=1}^{nb}(RMSE(MS_i, F_i))^2} \quad (20)$$

where nb is the number of band; l and p are the spatial resolution of the upsampled MS and PAN images.

4.2.5 Relative average spectral error metric (RASE)

It is computed using the RMSE. Its formulas are given as follows:

$$RASE = \frac{100}{E(MS_i)}\sqrt{\sum_{i=1}^{nb}(RMSE(MS_i, F_i))^2} \quad (21)$$

where $E(MS_i)$ is the mean of MS_i band; nb is the number of band.

4.2.6 The results comparison

Different results obtained from various methods by each measure are shown in Table 1.

Table 1. The result of different metrics using on IKONOS and Pléiades images

		CC	SCC	RMSE	ERGAS	RASE
	Reference	1	1	0	0	0
IKONOS Image	PCA	0.9370	0.9916	38.9555	3.2878	12.9149
	GIHS-SRF	0.9211	0.9897	62.2564	4.5010	19.8852
	GIHS	0.9062	0.9917	52.6836	4.7690	17.1510
	Brovey	0.9167	0.9855	41.0321	3.3154	13.2905
	WT	0.9337	0.9267	38.1028	3.1139	12.3211
	GSA	0.9435	0.9921	39.0302	3.3080	13.0204
	FUFSER	0.9462	0.9203	35.9992	3.0649	12.6694
	Proposed	**0.9491**	**0.9937**	**34.4829**	**2.8254**	**11.2468**
Pléiades Image	PCA	0.8112	0.9791	46.8343	5.8527	26.0701
	GIHS-SRF	0.7953	**0.9920**	65.0675	8.7538	32.5661
	GIHS	0.7528	0.9917	77.0054	13.8752	38.8216
	Brovey	0.8101	0.9852	42.1642	5.2367	21.8163
	WT	0.8685	0.8052	35.4696	4.7299	17.8457
	GSA	0.8548	0.9914	38.8243	5.2223	19.7607
	FUFSER	0.8802	0.8994	34.6084	5.6610	19.2322
	Proposed	**0.9172**	0.9864	**29.5591**	**3.6699**	**15.5703**

The results of the best values are illustrated in bold.

From Table 1, for IKONOS image, it can be seen that the proposed method gives the best values of all metrics. This indicates that the proposed method can inject the spatial information of the PAN and maintain the spectral information of the MS images well than other methods for IKONOS images.

From Table 1, for Pléiades image, it can be seen that the proposed method gives the best values of all metrics except for the SCC. However, it gives an exactable values for this metrics. This indicates that the proposed method has good results for Pléaides images.

Overall, the proposed method has a good equilibrium between the spectral and the spatial information on the all used images.

5. CONCLUSIONS

In this work, we proposed a novel image fusion method. We estimated the amount of spatial details to be transferred from the PAN image into the MS images. To do this operation, we utilized global and local parameters. The global parameters are computed by FFO technique while the local parameters are computed by the local entropy. The experiments were tested on IKONOS and Pléiades images. Five evaluation metrics were computed to evaluate both the spatial and spectral qualities of the merged images. The results showed that the proposed method have better performances than other methods in terms of spectral and spatial quality of the fused image.

REFERENCES

[1] Lari SN, Yazdi M. (2016). Improved IHS pan-sharpening method based on adaptive injection of à trous wavelet decomposition. International Journal of Signal Processing, Image Processing and Pattern Recognition. 9(3): 291-308. https://doi.org/10.14257/ijsip.2016.9.3.26

[2] Zhang Y. (2004). Understanding image fusion. Photogramm. Eng. Remote Sens. 70(6): 657-661.

[3] Thomas C, Ranchin T, Wald L, Chanussot J. (2008). Synthesis of multispectral images to high spatial resolution: a critical review of fusion methods based on remote sensing physics. IEEE Trans. Geosci. and Remote Sens. 46(5): 1301-1312. https://doi.org/10.1109/TGRS.2007.912448

[4] Panchal1 S, Thakker R. (2015). Implementation and comparative quantitative assessment of different multispectral image pansharpening approaches. Signal & Image Processing: An International Journal (SIPIJ). 6(5). https://doi.org/10.5121/sipij.2015.6503

[5] Mu T, Su SC, Shyu HS, Huang S. (2001). A new look at IHS like image fusion methods. Info. Fusion. 2(3):177-186. https://doi.org/10.1016/S1566-2535(01)00036-7

[6] Hanping M, Yancheng Z, Xinzhong W. Fusion algorithm for multi-sensor images based on PCA and lifting wavelet transformation. New Zealand Journal of Agricultural 50(5): 667-671. https://doi.org/10.1080/00288230709510336

[7] Akoguz A. (2014) Pansharpening of multispectral images using filtering in Fourier domain. image and signal processing for remote sensing. Proceeding of 2014, SPIE 9244, 92441X. https://doi.org/10.1117/12.2067255.

[8] Otazu X, González-Audícana M, Fors O. (2005). Introduction of sensor spectral response into image fusion methods. IEEE Trans. Geosci. Remote Sens. 43(10): 2376-2385. https://doi.org/10.1109/TGRS.2005.863299

[9] Ghellab A, Belbachir MF. (2013) Efficient image fusion method based on the Fourier transform by introducing sensor spectral response. J. Appl. Remote Sens. 7(1): 073552. https://doi.org/10.1117/1.JRS.7.073552

[10] Wang Z, Bovik AC, Sheik HR, Simoncelli EP. (2014). Image Quality Assessment: From error visibility to structural similarity. IEEE Transactions on Image Processing. 13(4): 600-612. https://doi.org/10.1109/TIP.2003.819861

[11] Zhou J, Tang BG, Ren XW. (2017) Research on prediction model for icing thickness of transmission lines based on BP neural network optimized with improved fruit fly algorithm. AMSE Journal-AMSE IIETA Publication 60: 255-269. https://doi.org/10.18280/ama_b.600116

[12] Pan W. (2012) A new fruit fly optimization algorithm Taking the financial distress model as an example. Knowledge-Based Systems 26: 69-74. https://doi.org/10.1016/j.knosys.2011.07.001

[13] Wang Z, Ziou D, Armenakis C, Li D, Li Q. (2005). A comparative analysis of image fusion methods. IEEE Trans. Geosci. Remote Sens. 43(6): 1391-1402. https://doi.org/10.1109/TGRS.2005.846874

[14] Park JH, Kang MG. (2004). Spatially adaptive multi-resolution multispectral image fusion. Int J Remote Sens 25(23): 5491-5508. https://doi.org/10.1080/01431160412331270830

[15] Choi J, Han D, Kim Y (2012). Context-adaptive pansharpening algorithm for high-resolution satellite imagery. Can J Remote Sensing 38(1): 109-124. https://doi.org/10.5589/m12-015

[16] Kim Y, Eo Y. (2011). Generalized IHS-based satellite imagery fusion using spectral response functions. ETRI J. 33(4): 497-505. https://doi.org/10.4218/etrij.11.1610.0042

[17] Roberts JW, Aardt JV, Ahmed F. (2008). Assessment of image fusion procedures using entropy, image quality, and multispectral classification. J Appl Remote Sens. 2(1): 023522. https://doi.org/10.1117/1.2945910

[18] Chavez PS, Kwarteng AW. (1989). Extracting spectral contrast in Landsat thematic mapper image data using selective principal component analysis. Photogrammetric Engineering and Remote Sensing. 55(3): 339-348.

[19] Vivone G, Alparone L, Chanussot J. (2015). A critical comparison among pan sharpening algorithms. IEEE Transactions on Geoscience and Remote Sensing 53(5): 2565-2586. https://doi.org/10.1109/TGRS.2014.2361734.

[20] Núñez J. (1999). Multiresolution-based image fusion with additive wavelet decomposition. IEEE Trans Geosci Remote Sens 37(3): 1204-1211.

[21] Aiazzi B, Baronti S, Selva M. (2007). Improving component substitution pansharpening through multivariate regression of MS+Pan data. IEEE Trans Geosci Remote Sens 45(10): 3230-3239. https://doi.org/10.1109/TGRS.2007.901007

[22] Palubinskas G. (2013) Fast, simple, and good pan-sharpening method. J. Appl. Remote Sens. 7(1): 073526. https://doi.org/10.1117/1.JRS.7.073526

[23] Srikanth B, Kumar H, Rao K. (2018) A robust approach for WSN localization for underground coal mine monitoring using improved RSSI technique. Mathematical Modelling of Engineering Problems 5(3): 225-231. https://doi.org/10.18280/mmep.050314

[24] Wald L, Ranchin T, Mangolini M. (1997) Fusion of satellite images of different spatial resolutions: Assessing the quality of resulting images. Amer Soc Photogramm Remote Sens. 63(6): 691-699.

[25] Wang Z, Bovik AC, Sheik HR, Simoncelli EP. (2004) Image Quality Assessment: From error visibility to structural similarity. IEEE Transactions on Image Processing 13(4): 600-612. https://doi.org/10.1109/TIP.2003.819861